

Supporting Information

Stable and luminescent cesium copper halide nanocrystals embedded in flexible polymer fibers for fabrication of down-converting WLEDs

*Manav Raj Kar,¹ Kajol Sahoo,¹ Ashutosh Mohapatra,¹ and Saikat Bhaumik^{1, 2, *}*

Characterization methods: UV-visible absorption spectra of NCs were recorded with a Shimadzu UV-2700 Spectrophotometer. Steady-state photoluminescence (PL) spectra were collected with Ocean Insight MAYA 2000 Pro high-sensitivity spectrometer using a 280 nm UV excitation source. X-Ray diffraction (XRD) analysis was carried out with the Bruker D8 diffractometer using Cu-K α ($\lambda=1.54$ Å) as incident radiation. Transmission electron microscopy (TEM) was recorded by Jeol-JEM-2010 microscope operated at 200 kV to determine the shape and size of the NCs. The Fourier Transform Infrared spectroscopy (FTIR) analysis was carried out using JASCO FT/IR-6600 Infrared Spectrometer to confirm the passivation of ligands around the NCs. The X-ray Photoelectron spectroscopy (XPS) analysis was carried out in an Omicron (series 0571) electron spectrometer to confirm the presence of elements in NCs. Fluorescence microscopy of NCs and fibers films was performed using a Nikon Eclipse Ci (Y-TV55) fluorescence microscope. Field emission scanning electron microscopy (FESEM) imaging of NCs and fibers films was recorded by JEOL JSM-7610F PLUS. The contact angle of NCs and fibers films was recorded using a Kyowa DME-211 contact angle meter.

Results and discussion:

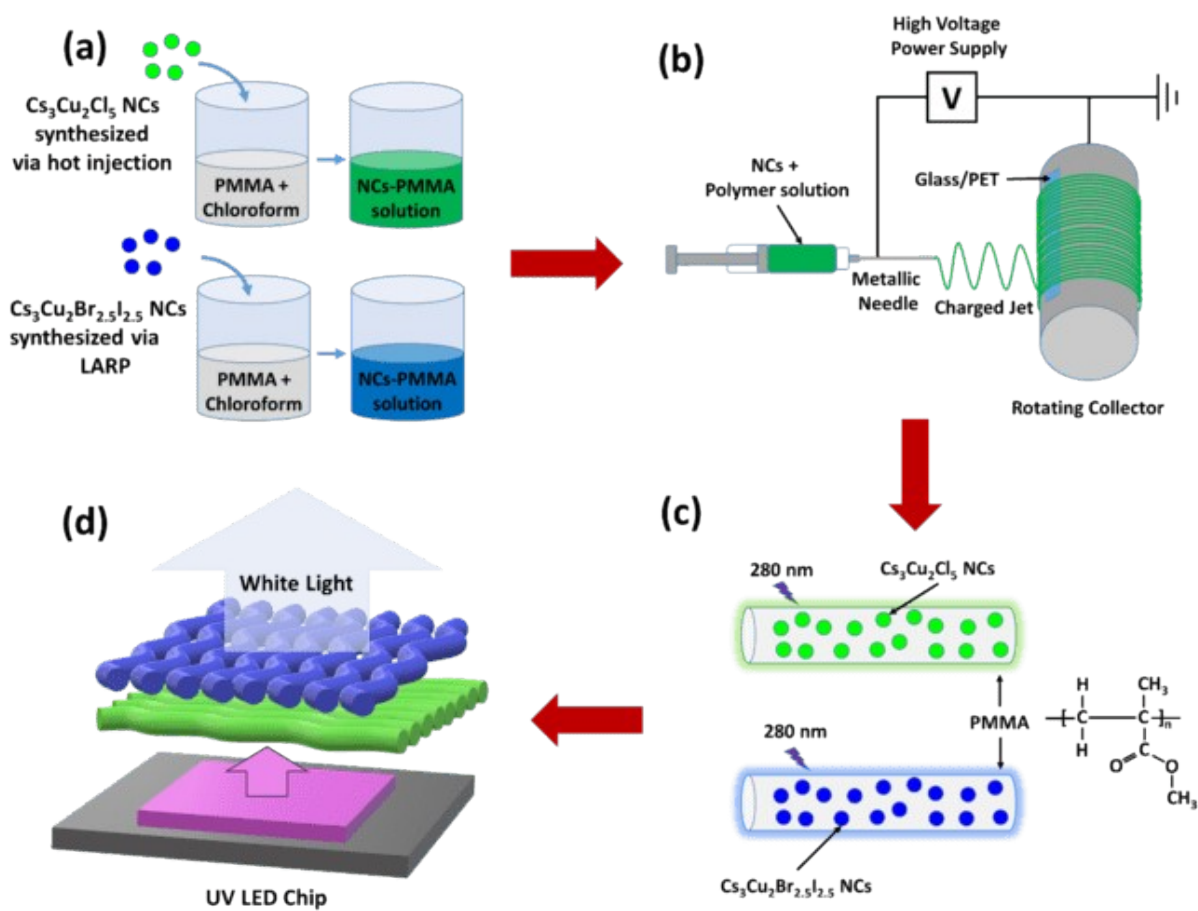


Fig. S1: (a-c) Schematic representing fabrication process of $\text{Cs}_3\text{Cu}_2\text{Cl}_5$ and $\text{Cs}_3\text{Cu}_2\text{Br}_{2.5}\text{I}_{2.5}$ @PMMA fibers via electrospinning process. (d) Schematic of the prototype down-converted WLED device.

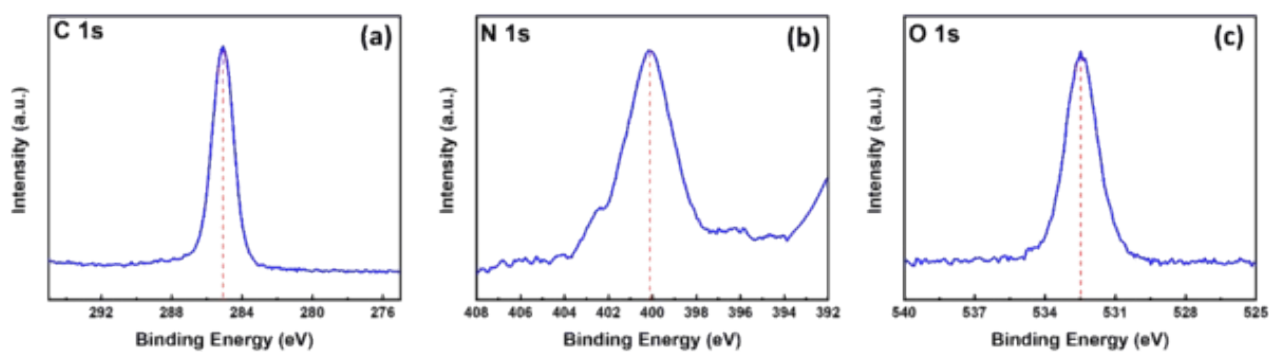


Fig. S2: High-Resolution XPS spectra of (a) C 1s, (b) N 1s, and (c) O 1s chemical states.

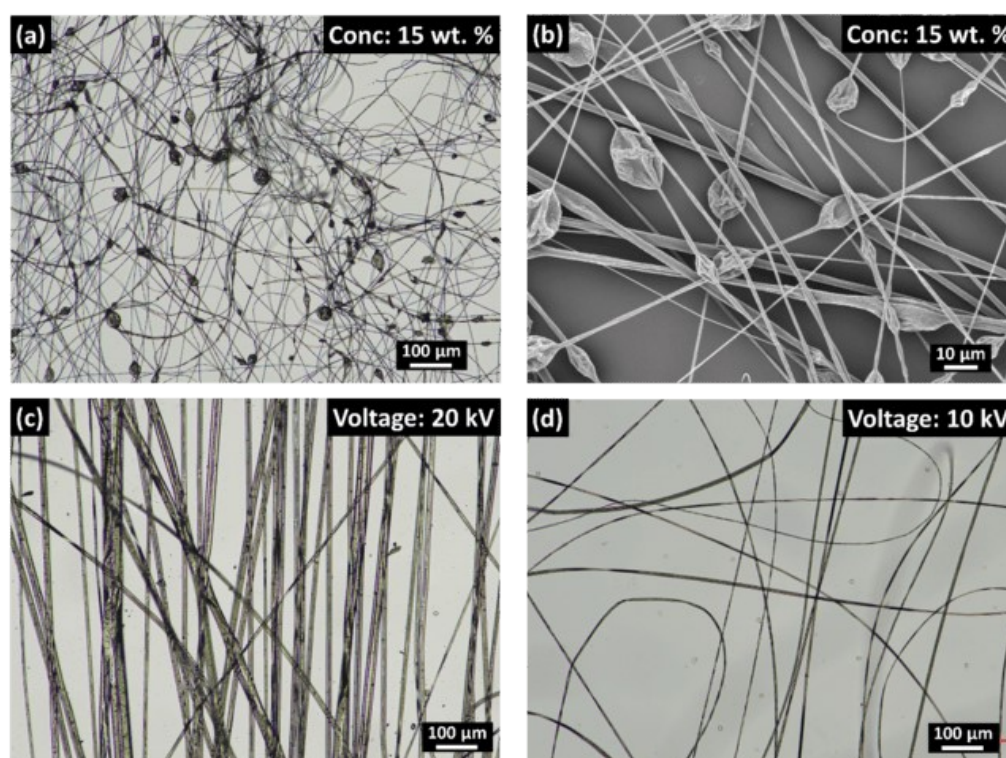


Fig. S3: (a) Flourescence microscope, and (b) FESEM images of PMMA fibers films fabricated from 15 wt. % PMMA/chloroform solution. Flourescence microscope images of the fibers films prepared with 20 wt. % PMMA/chloroform solution while operation voltage was maintained at (c) 20 kV, and (d) 10 kV.

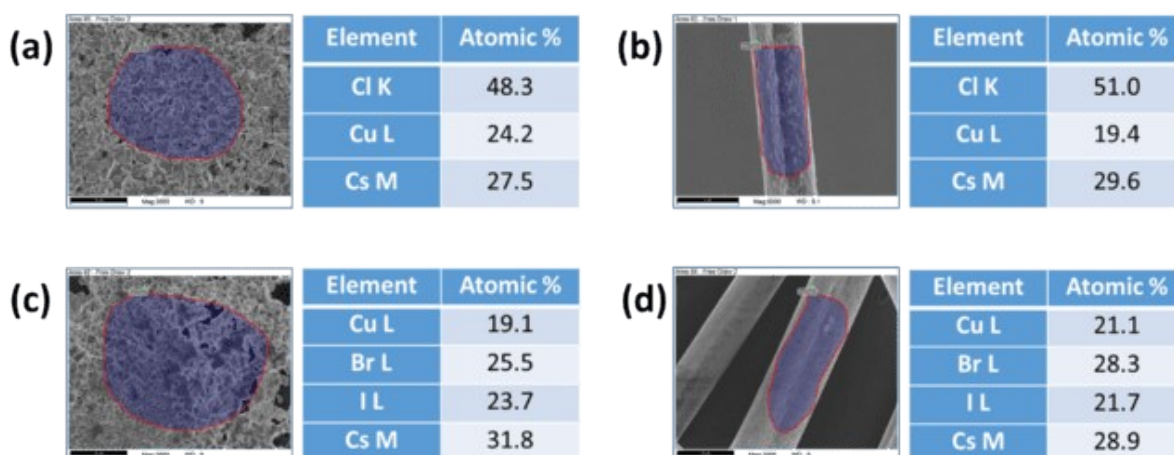


Fig. S4: EDS data obtained from FESEM images of (a) $\text{Cs}_3\text{Cu}_2\text{Cl}_5$ NCs, (b) $\text{Cs}_3\text{Cu}_2\text{Cl}_5$ @PMMA fiber, (c) $\text{Cs}_3\text{Cu}_2\text{Br}_{2.5}\text{I}_{2.5}$ NCs, and (d) $\text{Cs}_3\text{Cu}_2\text{Br}_{2.5}\text{I}_{2.5}$ @PMMA fiber films.

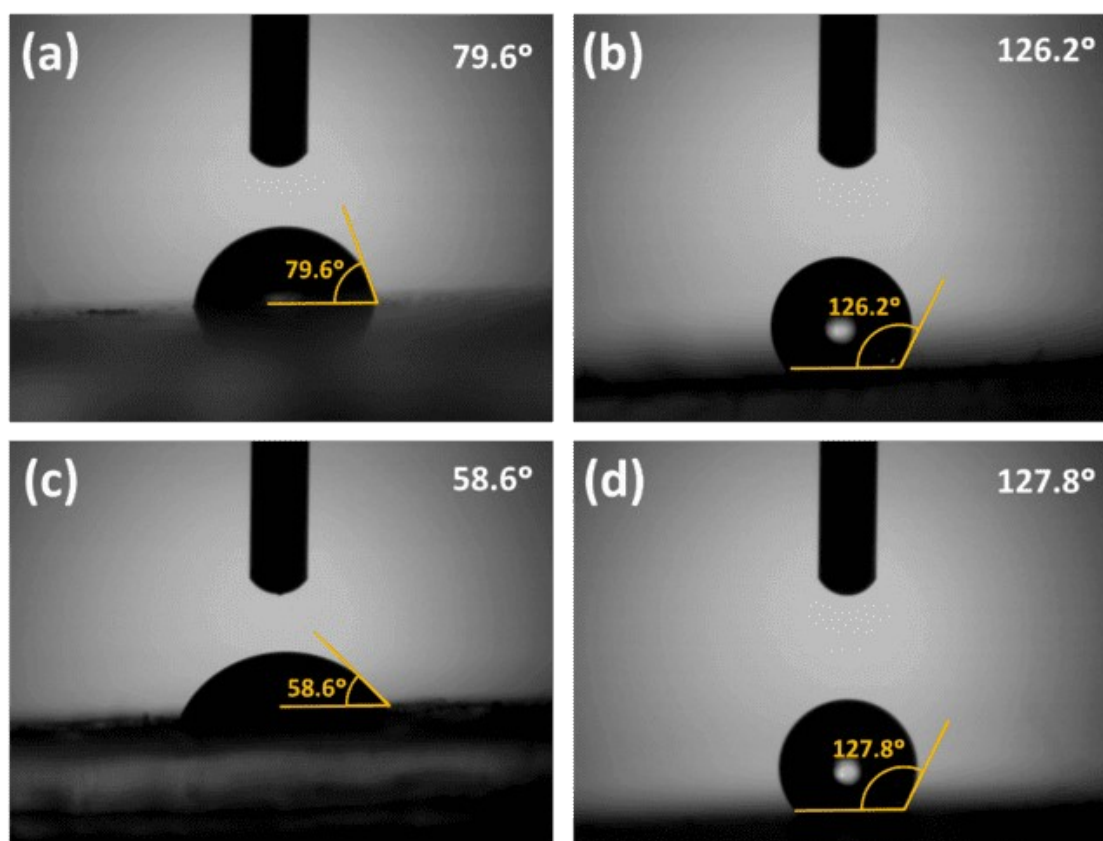


Fig. S5: Images showing contact angle of a water droplet over film of (a) $\text{Cs}_3\text{Cu}_2\text{Cl}_5$ NCs, (b) $\text{Cs}_3\text{Cu}_2\text{Cl}_5$ @PMMA fiber, (c) $\text{Cs}_3\text{Cu}_2\text{Br}_{2.5}\text{I}_{2.5}$ NCs, and (d) $\text{Cs}_3\text{Cu}_2\text{Br}_{2.5}\text{I}_{2.5}$ @PMMA fiber films, respectively.

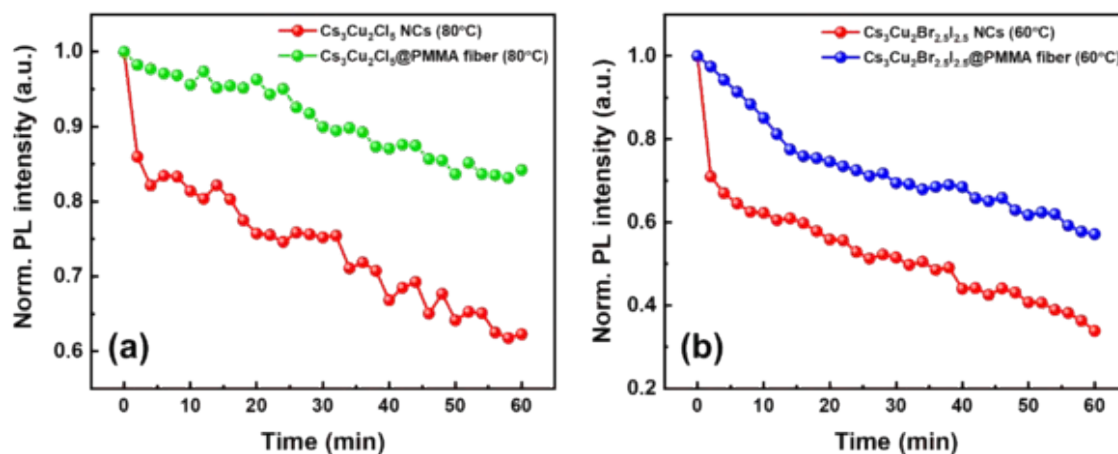


Fig. S6: The relative change in PL intensities of (a) $\text{Cs}_3\text{Cu}_2\text{Cl}_5$ NCs and $\text{Cs}_3\text{Cu}_2\text{Cl}_5$ @PMMA fibers films, and (b) $\text{Cs}_3\text{Cu}_2\text{Br}_{2.5}\text{I}_{2.5}$ NCs and $\text{Cs}_3\text{Cu}_2\text{Br}_{2.5}\text{I}_{2.5}$ @PMMA fibers films while kept on a hot plate over different time intervals as shown in legends.

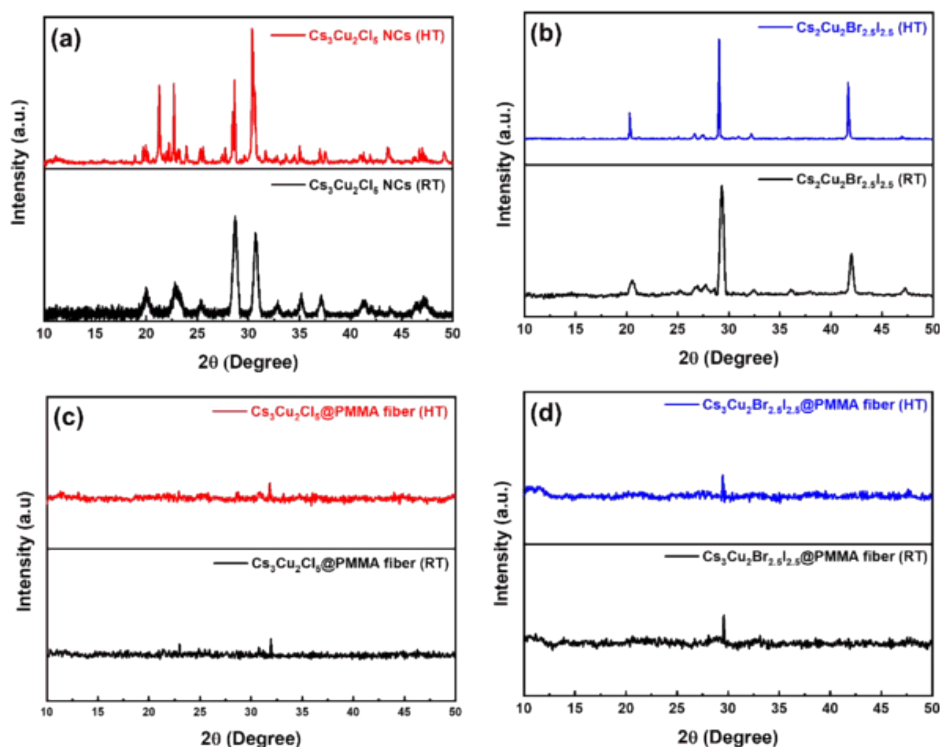


Fig. S7: Staked XRD patterns of (a) $\text{Cs}_3\text{Cu}_2\text{Cl}_5$ NCs, (b) $\text{Cs}_3\text{Cu}_2\text{Br}_{2.5}\text{I}_{2.5}$ NCs, (c) $\text{Cs}_3\text{Cu}_2\text{Cl}_5$ @PMMA fiber, and (d) $\text{Cs}_3\text{Cu}_2\text{Br}_{2.5}\text{I}_{2.5}$ @PMMA fiber films before (black line) and after thermal treatment (red and blue lines), as represented in legends.

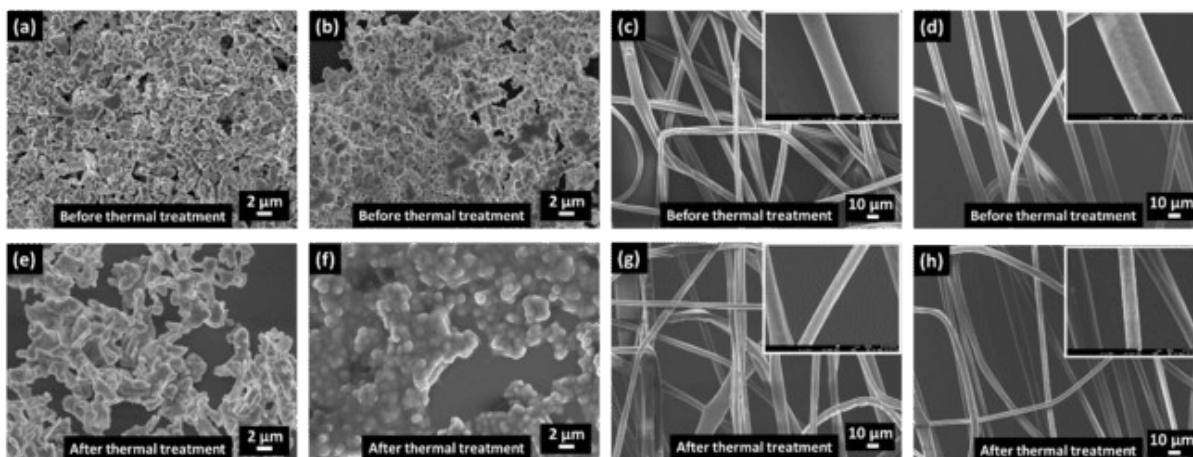


Fig. S8: FESEM images of (a) $\text{Cs}_3\text{Cu}_2\text{Cl}_5$ NCs, (b) $\text{Cs}_3\text{Cu}_2\text{Br}_{2.5}\text{I}_{2.5}$ NCs, (c) $\text{Cs}_3\text{Cu}_2\text{Cl}_5$ @PMMA fiber, (d) $\text{Cs}_3\text{Cu}_2\text{Br}_{2.5}\text{I}_{2.5}$ @PMMA fiber films. FESEM images of (e) $\text{Cs}_3\text{Cu}_2\text{Cl}_5$ NCs, (f) $\text{Cs}_3\text{Cu}_2\text{Br}_{2.5}\text{I}_{2.5}$ NCs, (g) $\text{Cs}_3\text{Cu}_2\text{Cl}_5$ @PMMA fiber, (h) $\text{Cs}_3\text{Cu}_2\text{Br}_{2.5}\text{I}_{2.5}$ @PMMA fiber films after thermal treatment. Inset: HR-FESEM images of respective fibers.

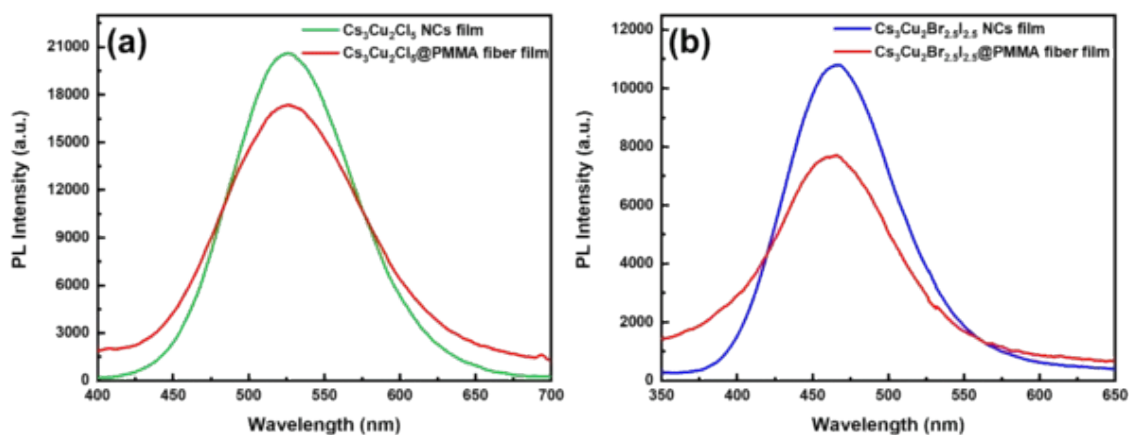


Fig. S9: PL spectra of (a) $\text{Cs}_3\text{Cu}_2\text{Cl}_5$ NCs and $\text{Cs}_3\text{Cu}_2\text{Cl}_5$ @PMMA fibers, and (b) $\text{Cs}_3\text{Cu}_2\text{Br}_{2.5}\text{I}_{2.5}$ NCs and $\text{Cs}_3\text{Cu}_2\text{Br}_{2.5}\text{I}_{2.5}$ @PMMA fibers films, as shown in legends.

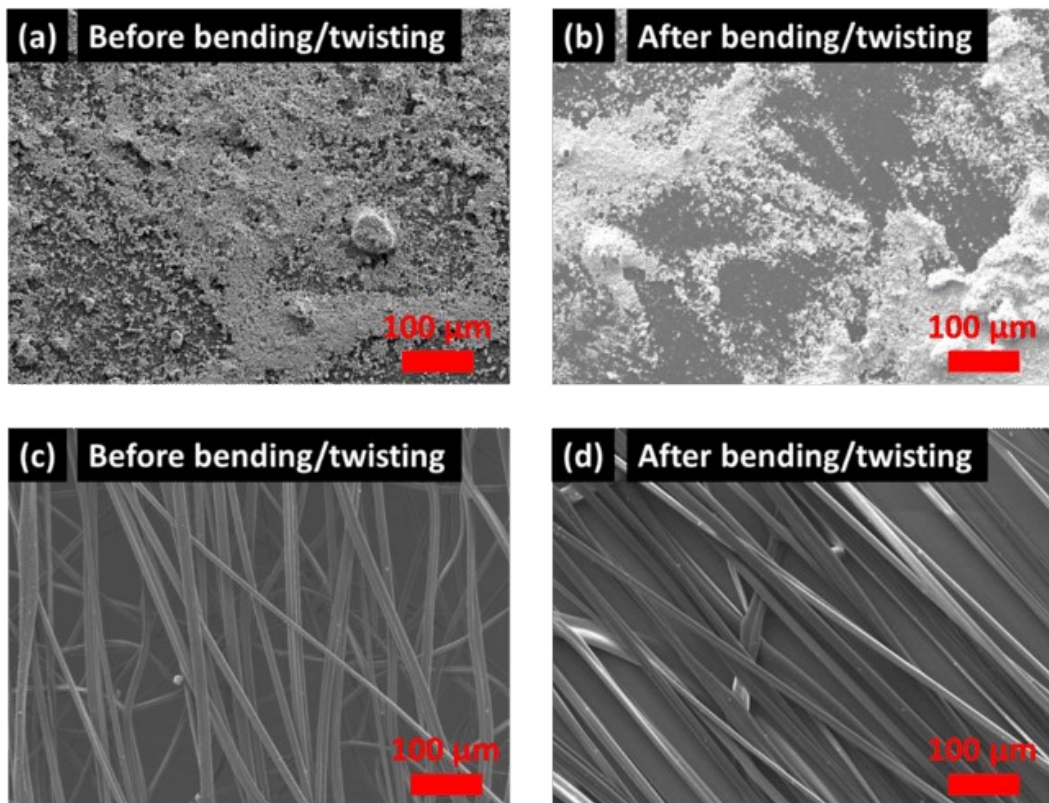


Fig. S10: FESEM images of (a) Cs₃Cu₂Cl₅ NCs films before bending/twisting, and (b) after bending/twisting. FESEM images of (c) Cs₃Cu₂Cl₅ @PMMA fiber films before bending/twisting, and (d) after bending/twisting.

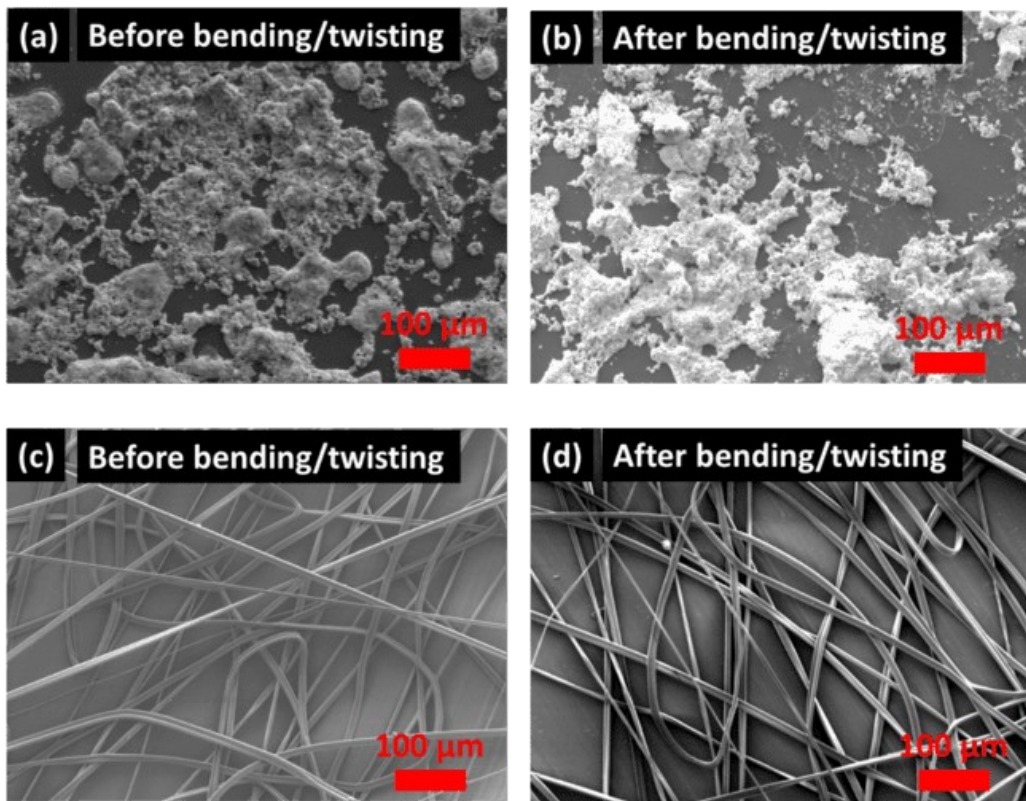


Fig. S11: FESEM images of (a) $\text{Cs}_3\text{Cu}_2\text{Br}_{2.5}\text{I}_{2.5}$ NCs films before bending/twisting, and (b) after bending/twisting. FESEM images of (c) $\text{Cs}_3\text{Cu}_2\text{Br}_{2.5}\text{I}_{2.5}$ @PMMA fiber films before bending/twisting, and (d) after bending/twisting.

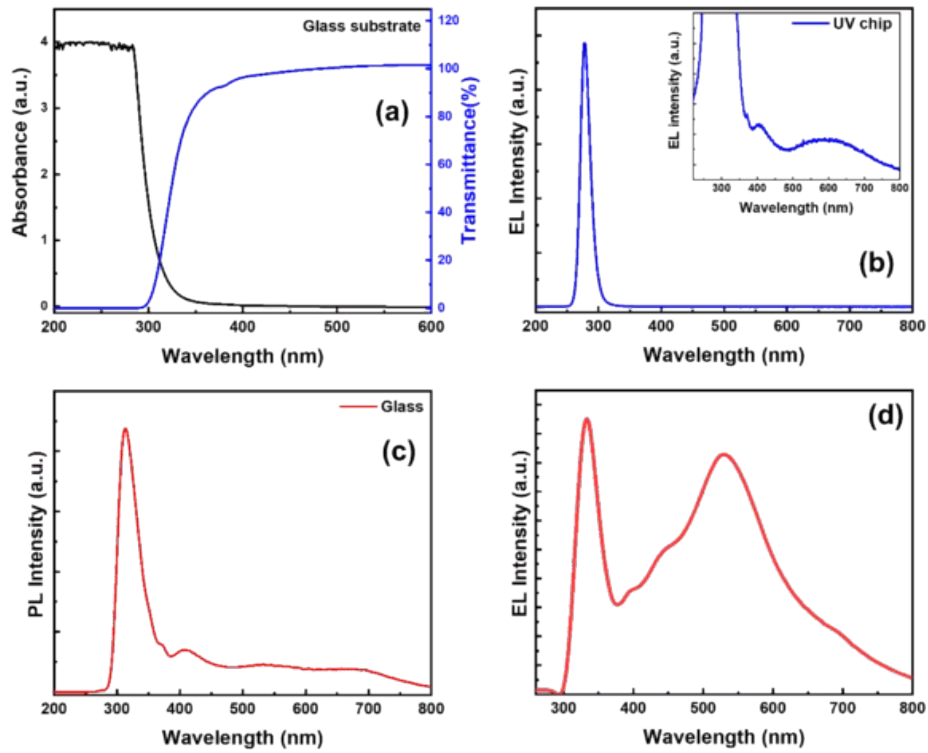


Fig. S12: (a) Absorption and transmission spectra of glass substrate. (b) EL spectrum of the UV LED chip. Inset: Zoomed EL spectrum of the chip. (c) PL spectrum of glass substrate. (d) EL spectrum of the WLED fabricated from NCs embedded fibers films.

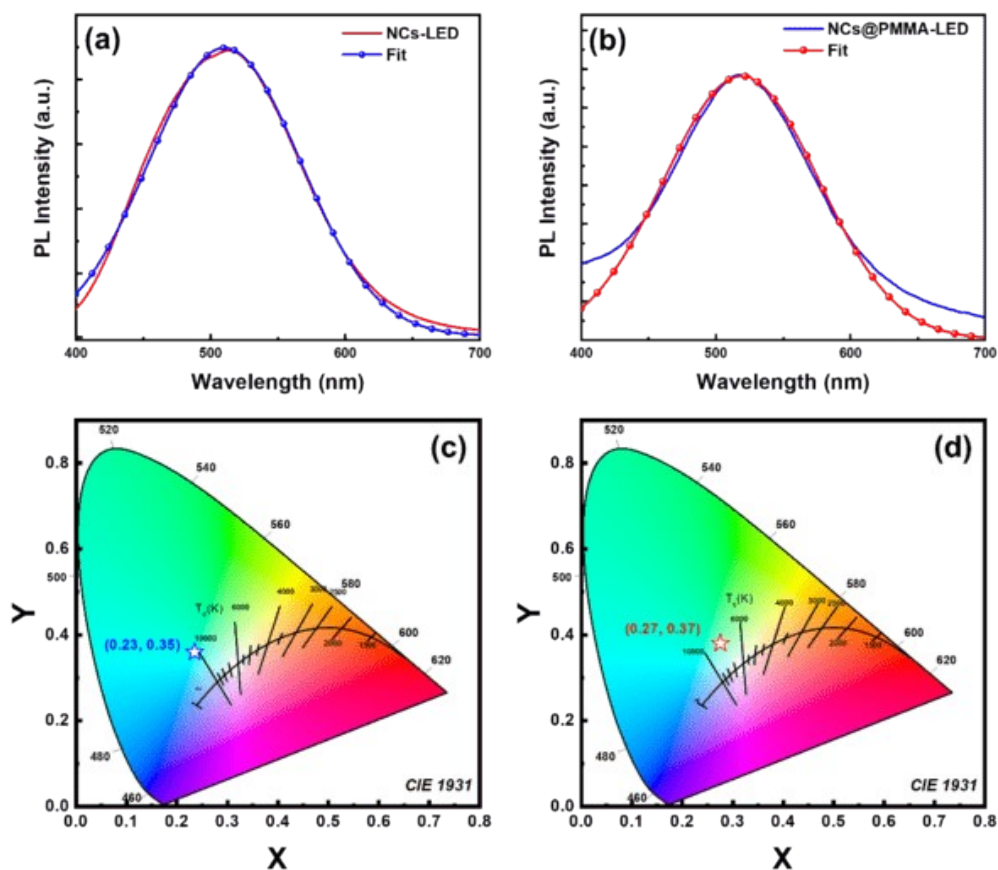


Fig. S13: Deconvoluted EL spectra of the color-converted LED for mixture of (a) bare NCs and (b) NCs@PMMA mixture films. Chromaticity coordinates of LED fabricated from (c) bare NCs films (blue outlined star) and (d) NCs@PMMA mixture films (red outlined star) according to 1931 CIE chromaticity diagram.